Accelerated Publication

THE JOURNAL OF BIOLOGICAL CHEMISTRY
Vol. 280, No. 20, Issue of May 20, pp. 19441–19444, 2005
© 2005 by The American Society for Biochemistry and Molecular Biology, Inc.
Printed in U.S.A.

Structural and Kinetic Analysis of the Substrate Specificity of Human Fibroblast Activation Protein α*[S]

Received for publication, March 4, 2005,
and in revised form, March 23, 2005
Published, JBC Papers in Press, April 4, 2005,
DOI 10.1074/jbc.C500092200

Kathleen Aertgeerts‡, Irena Levin, Lihong Shi, Gyorgy P. Snell, Andy Jennings, G. Sridhar Prasad, Yanming Zhang, Michelle L. Kraus, Shant Salakian, Vandana Sridhar, Robert Wijnands, and Mike G. Tennant

From Takeda San Diego, Inc., San Diego, California 92121

Fibroblast activation protein α (FAPα) is highly expressed in epithelial cancers and has been implicated in extracellular matrix remodeling, tumor growth, and metastasis. We present the first high resolution structure for the apoenzyme as well as kinetic data toward small dipeptide substrates. FAPα exhibits a dipeptidyl peptidase IV (DPPIV)-like fold, featuring an α/β-hydrolase domain and an eight-bladed β-propeller domain. Known DPPIV dipeptides are cleaved by FAPα with an ~100-fold decrease in catalytic efficiency compared with DPPIV. Moreover, FAPα, but not DPPIV, possesses endopeptidase activity toward N-terminal benzyloxycarbonyl (Z)-blocked peptides. Comparison of the crystal structures of FAPα and DPPIV revealed one major difference in the vicinity of the Glu motif (Glu^{203}-Glu^{204} for FAPα; Glu^{205}-Glu^{206} for DPPIV) within the active site of the enzyme. Ala^{657} in FAPα, instead of Asp^{663} as in DPPIV, reduces the acidity in this pocket, and this change could explain the lower affinity for N-terminal amines by FAPα. This hypothesis was tested by kinetic analysis of the mutant FAPα/A657D, which shows on average an ~60-fold increase in the catalytic efficiency, as measured by k_{cat}/K_m, for the cleavage of dipeptide substrates. Furthermore, the catalytic efficiency of the mutant is reduced by ~350-fold for cleavage of Z-Gly-Pro-7-amino-4-methylcoumarin. Our data provide a clear understanding of the molecular determinants responsible for the substrate specificity and endopeptidase activity of FAPα.

FAPα[1] is expressed on reactive stromal fibroblasts in over 90% of common human epithelial cancers (1), in granulation tissue of healing wounds, and in bone and soft tissue sarcomas (2). Expression of FAPα is not detected in fibroblasts of benign epithelial tumors or normal adult tissues.

FAPα is a type II transmembrane serine protease and has both *in vitro* dipeptidyl peptidase activity capable of cleaving N-terminal dipeptides from polypeptides (3) and collagenolytic activity capable of degrading gelatin and type I collagen (4, 5). Both functions utilize a common active site in FAPα (5). It has been suggested that FAPα promotes tumor growth and proliferation (4–7). In contrast, other studies have suggested that FAPα has tumor suppressor activity (8–10) and showed that this activity is independent of its enzymatic activity (10). The role of FAPα in tumor growth and invasion and the exact molecular mechanisms the enzyme utilizes remains unknown.

The closest homolog of FAPα is dipeptidyl peptidase IV (DPPIV). In contrast to FAPα, DPPIV is ubiquitously expressed and plays a role in various processes such as T cell co-stimulation, chemokine biology, glucose metabolism, and tumorigenesis (11, 12). Interestingly, an active DPPIV/FAPα heterodimer has been identified on the surface of migratory connective tissue cells and contributes to cell migration necessary for connective tissue repair (13, 14).

To investigate the molecular determinants that are responsible for the substrate specificity of FAPα, we solved the crystal structure of the extracellular domain and measured steady state catalytic parameters for various dipeptide substrates. We also used site-directed mutagenesis to confirm the importance of active site residue Ala^{657} in catalysis.

MATERIALS AND METHODS

Enzyme Expression and Purification—The cDNA encoding human FAPα was isolated by PCR from IMAGE clone 4731931 (ATCC 6670182). The extracellular domain of FAPα (residues 27–760) was cloned into a modified pFastBacHTb vector (Invitrogen). The final construct contains the coding sequence for a baculovirus gp67 signal peptide followed by residues 27–760 of FAPα and a His_6 tag. The theoretical molecular mass for the final expressed protein is 90 kDa. Human DPPIV was cloned and expressed as described previously (15). PCR-based site-directed mutagenesis was performed to generate the single amino acid substitutions FAPα/A657D and DPPIV/D663A using the constructs of the respective wild-type forms. Expression and purification of all enzymes was performed following the protocol as described previously (15).

Crystallization and Structure Determination—Diffraction quality crystals were obtained at 4 °C using Syrrx's automated Nanovolume Crystallisation® technology (16). The reservoir solution was 0.05 M CHES, pH 9.5, 22% polyethylene glycol 6000, and 1.26 M LiCl. Crystals appeared in about 5 days and grew to a maximum size within 7–10 days. For x-ray data collection, crystals were flash-frozen at 100 K using 25% v/v ethylene glycol as a cryoprotectant. Data were collected at beamline 5.0.3 (17) of the Advanced Light Source (ALS) and integrated and scaled using HKL2000 (18). Initial phases were obtained by molecular replacement using the program MOLREP (19). The coordinates of human DPPIV (Protein Data Bank entry 1R9M) were used as a search model (15). The highest solution from the translation function was subjected to rigid body refinement followed by maximum likelihood refinement as implemented in REFMAC (20). Rigid body refinement and torsional dynamics refinement were followed by multiple rounds of

* The costs of publication of this article were defrayed in part by the payment of page charges. This article must therefore be hereby marked "*advertisement*" in accordance with 18 U.S.C. Section 1734 solely to indicate this fact.

The atomic coordinates and structure factors (code 1Z68) have been deposited in the Protein Data Bank, Research Collaboratory for Structural Bioinformatics, Rutgers University, New Brunswick, NJ (http://www.rcsb.org/).

[S] The on-line version of this article (available at http://www.jbc.org) contains a supplemental table and figure.

‡ To whom correspondence should be addressed: Takeda San Diego, Inc., 10410 Science Center Dr., San Diego, CA 92121. Tel.: 858-731-3519; Fax: 858-550-0526; E-mail: kaertgeerts@takedasd.com.

[1] The abbreviations used are: FAPα, fibroblast activation protein α; DPPIV, dipeptidyl peptidase IV; Z, benzyloxycarbonyl; AFC, 7-amino-4-trifluoromethylcoumarin; AMC, 7-amino-4-methylcoumarin; CHES, 2-(cyclohexylamino)ethanesulfonic acid.

This is an Open Access article under the CC BY license.

Johns Hopkins University EX2034
GE Healthcare v. Johns Hopkins
IPR2026-00069

manual building with Xfit (21). All stages of model refinement were carried out with bulk solvent correction and anisotropic scaling.

Determination of Catalytic Activity—Kinetic parameters of DPPIV and FAPα for four different substrates were determined at room temperature using varying concentrations of the substrate in 100 μl of 20 mM Tris, pH 7.4, 20 mM KCl, 0.1 mg/ml bovine serum albumin, and 1% Me_2SO in 96-well half-area plates. Initial rates were monitored at E_x 400 nm and E_m 505 nm for 7-amino-4-trifluoromethycoumarin (AFC) substrate and at E_x 375 nm and E_m 460 nm for 7-amino-4-methylcoumarin (AMC) substrate using Molecular Devices SpectraMax Gemini. Assays were performed in duplicate for each substrate. MDL data analysis toolbox was used for analysis of Michaelis-Menten kinetic parameters.

RESULTS AND DISCUSSION

Overall Structure of FAPα—The asymmetric unit is composed of a homodimer with approximate dimensions of 60 × 80 × 125 Å (Fig. 1). The final R and R_{free} values of the refined model are 0.22 and 0.28, respectively. Additional information on the data collection and refinement statistics is provided in the supplemental material. Each subunit contains two topologically distinct domains: the β-propeller (residues 54–492) and the α/β-hydrolase domain (residues 27–53 and 493–760). Eight blades form the β-propeller domain with each blade comprising a three- or four-stranded antiparallel β-sheet. The organization of the blades in the propeller domain results in the formation of a central pore that has a length of ~27 Å and a diameter of ~14 Å.

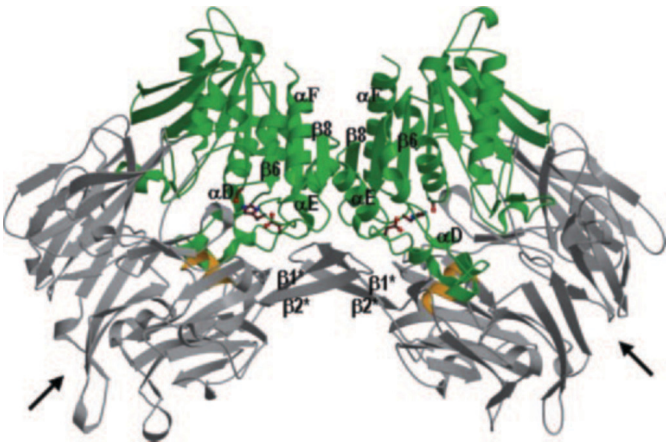


FIG. 1. **Ribbon diagram representing the overall structure of the FAPα dimer.** The β-propeller domain and α/β-hydrolase domain are shown in *gray* and *green*, respectively. The dimer is viewed perpendicular to its 2-fold dyad axis. Active site residues Ser^{624}, Asp^{702}, and His^{734} are represented in *ball-and-stick* representations. The α-helix containing the Glu motif is indicated in *yellow*. *Arrows* indicate the direction of the central pore. The figure was made using the programs MOLSCRIPT (22) and Raster3D (23).

The FAPα catalytic triad is composed of residues Ser^{624}, Asp^{702}, and His^{734} and is located at the interface of the β-propeller and the α/β-hydrolase domain (Fig. 1). The active site is accessible in two ways: through a central hole formed by the eight blades of the β-propeller domain or through a cavity formed between the β-propeller and the hydrolase domain. The side opening has a diameter of ~24 Å in contrast to the narrower β-propeller opening (~14 Å).

FAPα has five potential *N*-linked glycosylation sites on asparagine residues 49, 92, 227, 314, and 679. Four are located in the β-propeller domain, and one is located in the hydrolase domain. We observed electron density for sugar residues for four of the five sites for subunit A and for all five sites of subunit B. The exact contribution of glycosylation to folding, dimerization, and catalysis is unclear.

Dimerization of FAPα is required for its catalytic function (5). The homodimer interface buries a total solvent-accessible area of ~1400 $Å^2$. The monomers are related by a 2-fold dyad axis. The dimer interface involves β8 of the peptidase central β-sheet, the last two α-helices (αE and αF), the loop between β6 and αD, and the anti-parallel β-sheet composed of β-strands β1* and β2* (Fig. 1).

FAPα and DPPIV have a sequence identity of 50% and root mean square difference values for the overlay of 713 residues were 1.01, 1.55, and 1.75 Å for the C-α, main chain, and all heavy atoms, respectively.

FAPα Dipeptidyl Peptidase Activity—Under physiological conditions, FAPα is involved in extracellular matrix degradation, but its physiological substrates remain unidentified. On the other hand, DPPIV is an exopeptidase implicated in the degradation of many chemokines, neuropeptides, and peptide hormones, and its kinetic properties toward various peptide substrates have been studied extensively (24–27). A series of fluorogenic substrates that contain a free N terminus and a Pro present in the penultimate position was used to compare the specific exopeptidase activity of FAPα with DPPIV. The k_{cat}/K_m values for cleavage of Gly-Pro (GP)-AFC, Ala-Pro (AP)-AFC, and GP-AMC by FAPα are much lower than 10^5 M^{-1} s^{-1} and are about 100 times lower compared with DPPIV.

To investigate the endopeptidase activity of both enzymes, we tested their catalytic activity toward the N-terminal blocked dipeptide substrate Z-GP-AMC. This substrate is hydrolyzed by FAPα with a k_{cat}/K_m of 5.3×10^4 M^{-1} s^{-1} but is resistant to cleavage by DPPIV (Table I).

TABLE I
Kinetic constants for the hydrolysis of chromogenic and fluorogenic dipeptide substrates by the wild-type form and point mutants of FAPα and DPPIV

The data represent the mean of two determinants, which differed by less than 15%. ND, non-determined.

	FAPα wt	DPPIV wt	FAPα/A647D	DPPIV/D663A
AP-AFC				
k_{cat} (s^{-1})	ND	24	20	54
K_m (μM)	>200	13	12	120
k_{cat}/K_m (M^{-1} s^{-1})	2.1×10^4	1.8×10^6	1.7×10^6	4.5×10^5
GP-AFC				
k_{cat} (s^{-1})	ND	42	22	ND
K_m (μM)	>200	84	95	>200
k_{cat}/K_m (M^{-1} s^{-1})	4.3×10^3	5.0×10^5	2.3×10^5	1.1×10^5
GP-AMC				
k_{cat} (s^{-1})	ND	25	14	63
K_m (μM)	>1000	50	100	540
k_{cat}/K_m (M^{-1} s^{-1})	3.0×10^3	5.0×10^5	1.4×10^5	1.2×10^5
Z-GP-AMC				
k_{cat} (s^{-1})	ND	ND	ND	ND
K_m (μM)	ND	ND	ND	ND
k_{cat}/K_m (M^{-1} s^{-1})	5.3×10^4	9.0	1.5×10^2	1.6×10^3

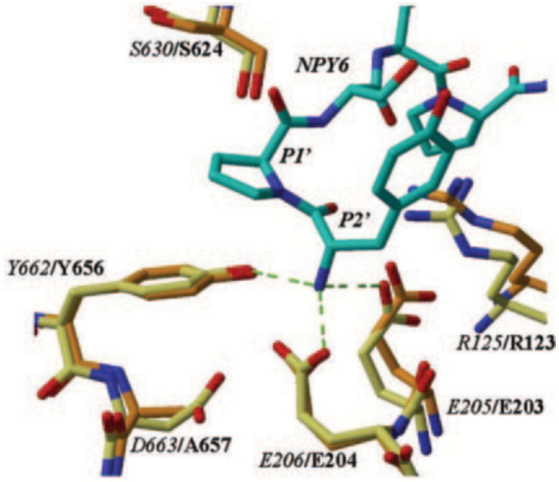


FIG. 2. **Superposition of FAPα with DPPIV showing a detailed view of the residues around the Glu motif.** The interactions in DPPIV between active site residues and the N terminus of the hexapeptide (*NPY6*, YPSKPD, *blue*), present in the crystal structure of DPPIV (*yellow*), are shown as *dashed lines* (15). Residues in FAPα are *orange*. Amino acid residues are labeled in *italic* and *bold* for DPPIV and FAPα, respectively. The figure was made using the program Xfit (21).

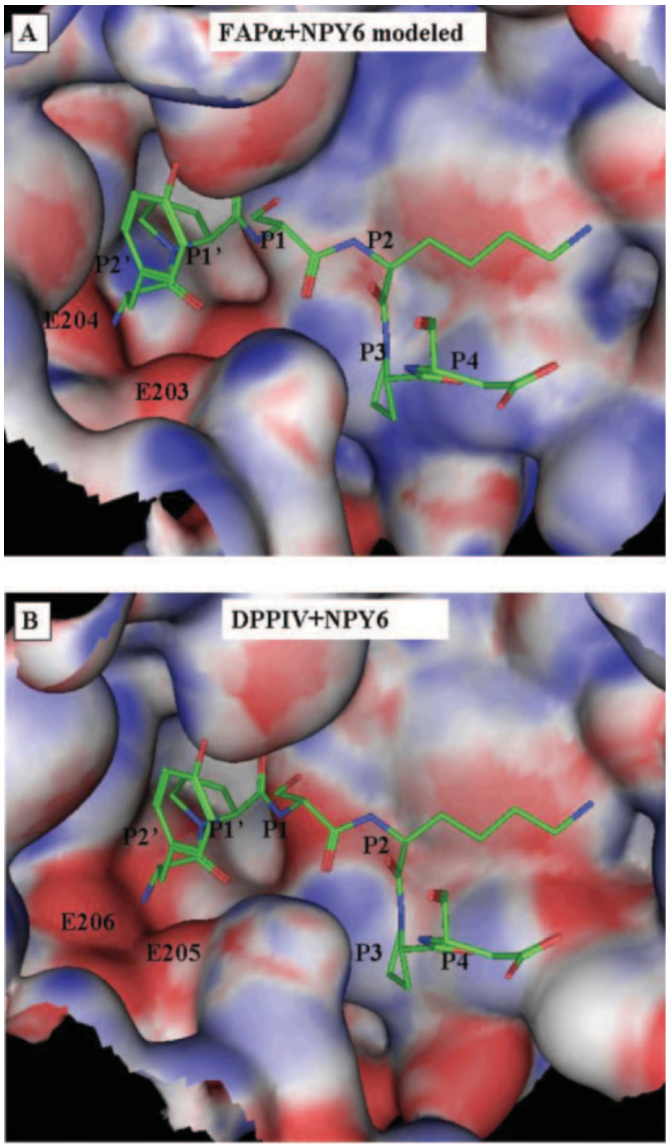


FIG. 3. **Surface representation of the active site of FAPα (*A*) and DPPIV (*B*).** The hexapeptide, NPY6 (YPSKPD), is represented as a *stick model* and is present in the crystal structure of DPPIV (15) and modeled in the structure of FAPα. The enzymes are represented as *solid surfaces*, *colors* represent positive and negative electrostatic potentials (*blue*, electropositive; *white*, neutral; *red*, electronegative). The relative difference in electrostatic effect around the Glu motif is represented in the figures. Residues of the decapeptide are numbered according to Berger and Schechter (28). The figures were made with MOE (Chemical Computing Group, 1010 Sherbrooke St. West, Suite 910, Montreal, Quebec H3A 2R, Canada).

Active Site and Substrate Binding Sites of FAPα—Structural comparison of the active sites of FAPα and DPPIV revealed similar S2-S2′ specificity pockets. The S1′ (numbered according to Berger and Schechter (28)) subsite in FAPα is flat and could accommodate most amino acids. The S2′ active site pocket is lined by Trp^{623} and Tyr^{745}. These residues would be expected to interact with large aliphatic side chains. The S1 specificity pocket in FAPα is a well defined hydrophobic pocket lined by Tyr^{625}, Val^{650}, Trp^{653}, Tyr^{656}, Tyr^{660}, and Val^{705}. This site optimally accommodates a proline residue. Large hydrophobic and aromatic residues can be modeled in the hydrophobic S2 pocket, defined by residues Arg^{123}, Phe^{350}, Phe^{351}, Tyr^{541}, Pro^{544}, Tyr^{625}, and Tyr^{660}.

The charged N-terminal end of substrate peptides is recognized by two glutamates (Glu^{203} and Glu^{204}). Both residues are located on an α-helix (residues 198–204) that protrudes from the β-propeller domain into the active site (Figs. 1 and 2). Glu^{204} has a single acid oxygen atom solvent-accessible and available for binding. The second acid oxygen atom is effectively buried in a hydrophobic pocket defined by Trp^{199}, Val^{200}, and Ala^{657} and probably forms a hydrogen bond, at least transiently, with the hydroxyl hydrogen of Tyr^{656}. The importance of the Glu motif (Glu^{205}-Glu^{206}) in DPPIV catalysis has been confirmed by single point mutants that abolish the enzyme aminopeptidase activity (29).

Detailed comparison between DPPIV and FAPα revealed a more pronounced negatively charged pocket in DPPIV due to the presence of Asp^{663} (corresponding residue in FAPα: Ala^{657}), which is in direct contact with Glu^{206} (Figs. 2 and 3). Asp^{663} in DPPIV pushes Glu^{206} further into the active site and exposes both acid oxygen atoms to the S2 pocket. This suggests that all three acidic residues may contribute to the recognition and anchoring of the free N terminus of peptide substrates (Figs. 2 and 3) in DPPIV.

Molecular Determinants for the Endopeptidase Activity of FAPα—To analyze the importance of Ala^{657} in FAPα and the corresponding residue Asp^{663} in DPPIV for the recognition of the N-terminal NH3+ group of substrate peptides, the mutant proteins, FAPα/A657D and DPPIV/D663A, were made and analyzed kinetically (Table I). The k_{cat}/K_m values for the cleavage by FAPα/A657D of GP-AFC, AP-AFC, and GP-AMC are on average increased by ~60-fold compared with the wild-type form of FAPα. The measured kinetic values (k_{cat}, K_m, and k_{cat}/K_m) are similar to the values obtained for wild-type DPPIV and confirm the importance of Ala^{657} in substrate recognition and enzyme catalysis. DPPIV/D663A shows an ~4-fold decrease in the catalytic efficiency for N-terminal dipeptide cleavage relative to the wild-type form of the enzyme. Replacement of Asp^{663} by an alanine turns DPPIV into a more efficient endopeptidase as demonstrated by the ability of this mutant to cleave Z-Gly-Pro-AMC. On the other hand, mutation of Ala^{657} to an Asp in FAPα reduces the k_{cat}/K_m for cleavage of Z-Gly-Pro-AMC by ~350-fold.

The structural and kinetic data described here provide a better understanding of the molecular mechanisms that determine the substrate specificity of FAPα. Comparison of our results with the reported structural and kinetic data on the related enzyme DPPIV reveals a reduced acidity in the active

site of FAPα due to the presence of Ala^{657} in FAPα instead of Asp^{663} as in DPPIV. As a consequence, the affinity for N-terminal peptides is reduced, and increased endopeptidase activity is observed.

Acknowledgments—We thank Steve Gwaltney, David Hosfield, Steve Kaldor, Marc Navre, David Weitz, and Keith Wilson for careful reading of the manuscript and helpful suggestions. We also thank ALS, which is supported by the Director, Office of Science, Office of Basic Energy Sciences, Materials Sciences Division, of the U. S. Department of Energy under Contract DE-AC03-76SF00098 at Lawrence Berkeley National Laboratory.

REFERENCES

1. Garin-Chesa, P., Old, L. J., and Rettig, W. J. (1990) *Proc. Natl. Acad. Sci. U. S. A.* **87,** 7235–7239
2. Rettig, W. J., Garin-Chesa, P., Beresford, H. R., Oettgen, H. F., Melamed, M. R., and Old, L. J. (1988) *Proc. Natl. Acad. Sci. U. S. A.* **85,** 3110–3114
3. Niedermeyer, J., Enenkel, B., Park, J. E., Lenter, M., Rettig, W. J., Damm, K., and Schnapp, A. (1998) *Eur. J. Biochem.* **254,** 650–654
4. Levy, M. T., McCaughan, G. W., Abbott, C. A., Park, J. E., Cunningham, A. M., Muller, E., Rettig, W. J., and Gorrell, M. D. (1999) *Hepatology* **29,** 1768–1778
5. Park, J. E., Lenter, M. C., Zimmermann, R. N., Garin-Chesa, P., Old, L. J., and Rettig, W. J. (1999) *J. Biol. Chem.* **274,** 36505–36512
6. Huber, M. A., Kraut, N., Park, J. E., Schubert, R. D., Rettig, W. J., Peter, R. U., and Garin-Chesa, P. (2003) *J. Invest. Dermatol.* **120,** 182–188
7. Cheng, J. D., Dunbrack, R. L., Jr., Valianou, M., Rogatko, A., Alpaugh, R. K., and Weiner, L. M. (2002) *Cancer Res.* **62,** 4767–4772
8. Rettig, W. J., Garin-Chesa, P., Healey, J. H., Su, S. L., Ozer, H. L., Schwab, M., Albino, A. P., and Old, L. J. (1994) *Cancer Res.* **53,** 385–392
9. Tsujimoto, H., Nishizuka, S., Redpath, J. L., and Stanbridge, E. J. (1999) *Mol. Carcinogen* **26,** 298–304
10. Ramirez-Montagut, T., Blachere, N. E., Sviderskaya, E. V., Bennett, D. C., Rettig, W. J., Garin-Chesa, P., and Houghton, A. N. (2004) *Oncogene* **23,** 5435–5446
11. De Meester, I., Korom, S., Van Damme, J., and Scharpe, S. (1999) *Immunol. Today* **20,** 367–375
12. Drucker, D. J. (2003) *Expert Opin. Investig. Drugs* **12,** 87–100
13. Scanlan, M. J., Raj, B. K., Calvo, B., Garin-Chesa, P., Sanz-Moncasi, M. P., Healey, J. H., Old, L. J., and Rettig, W. J. (1994) *Proc. Natl. Acad. Sci. U. S. A.* **91,** 5657–5661
14. Ghersi, G., Dong, H., Goldstein, L. A., Yeh, Y., Hakkinen, L., Larjava, H. S., and Chen, W. T. (2002) *J. Biol. Chem.* **277,** 29231–29241
15. Aertgeerts, K., Ye, S., Tennant, M. G., Kraus, M. L., Rogers, J., Sang, B. C., Skene, R. J., Webb, D. R., and Prasad, G. S. (2004) *Protein Sci.* **13,** 412–421
16. Hosfield, D., Palan, J., Hilgers, M., Scheibe, D., McRee, D. E., and Stevens, R. C. (2003) *J. Struct. Biol.* **142,** 207–217
17. Snell, G., Cork, C., Nordmeyer, R., Cornell, E., Meigs, G., Yegian, D., Jaklevic, J., Jin, J., Stevens, R. C., and Earnest, T. (2004) *Structure* **12,** 537–546
18. Otwinowski, Z., and Minor, W. (1997) *Methods Enzymol.* **276,** 307–326
19. Vagin, A., and Teplyakov, A. (1997) *J. Appl. Crystallogr.* **30,** 1022–1025
20. Murshudov, G. N., Vagin, A. A., and Dodson, E. J. (1997) *Acta Crystallogr. Sect. D* **53,** 240–255
21. McRee, D. E. (1999) *J. Struct. Biol.* **125,** 156–165
22. Kraulis, P. J. (1991) *J. Appl. Crystallogr.* **24,** 946–950
23. Merritt, E. A., and Bacon, D. J. (1997) *Methods Enzymol.* **277,** 505–524
24. Lambeir, A. M., Proost, P., Durinx, C., Bal, G., Senten, K., Augustyns, K., Scharpe, S., Van Damme, J., and De Meester, I. (2001) *J. Biol. Chem.* **276,** 29839–29845
25. Lambeir, A. M., Durinx, C., Proost, P., Van Damme, J., Scharpe, S., and De Meester, I. (2001) *FEBS Lett.* **507,** 327–330
26. Lambeir, A. M., Proost, P., Scharpe, S., and De Meester, I. (2002) *Biochem. Pharmacol.* **64,** 1753–1756
27. Zhu, L., Tamvakopoulos, C., Xie, D., Dragovic, J., Shen, X., Fenyk-Melody, J. E., Schmidt, K., Bagchi, A., Griffin, P. R., Thornberry, N. A., and Sinha Roy, R. (2003) *J. Biol. Chem.* **278,** 22418–22423
28. Berger, A., and Schechter, I. (1970) *Philos. Trans. R. Soc. Lond. B Biol. Sci.* **257,** 249–264
29. Abbott, C. A., McCaughan, G. W., and Gorrell, M. D. (1999) *FEBS Lett.* **458,** 278–284

SUPPLEMENTAL MATERIAL

X-ray data collection and refinement statistics for FAPα

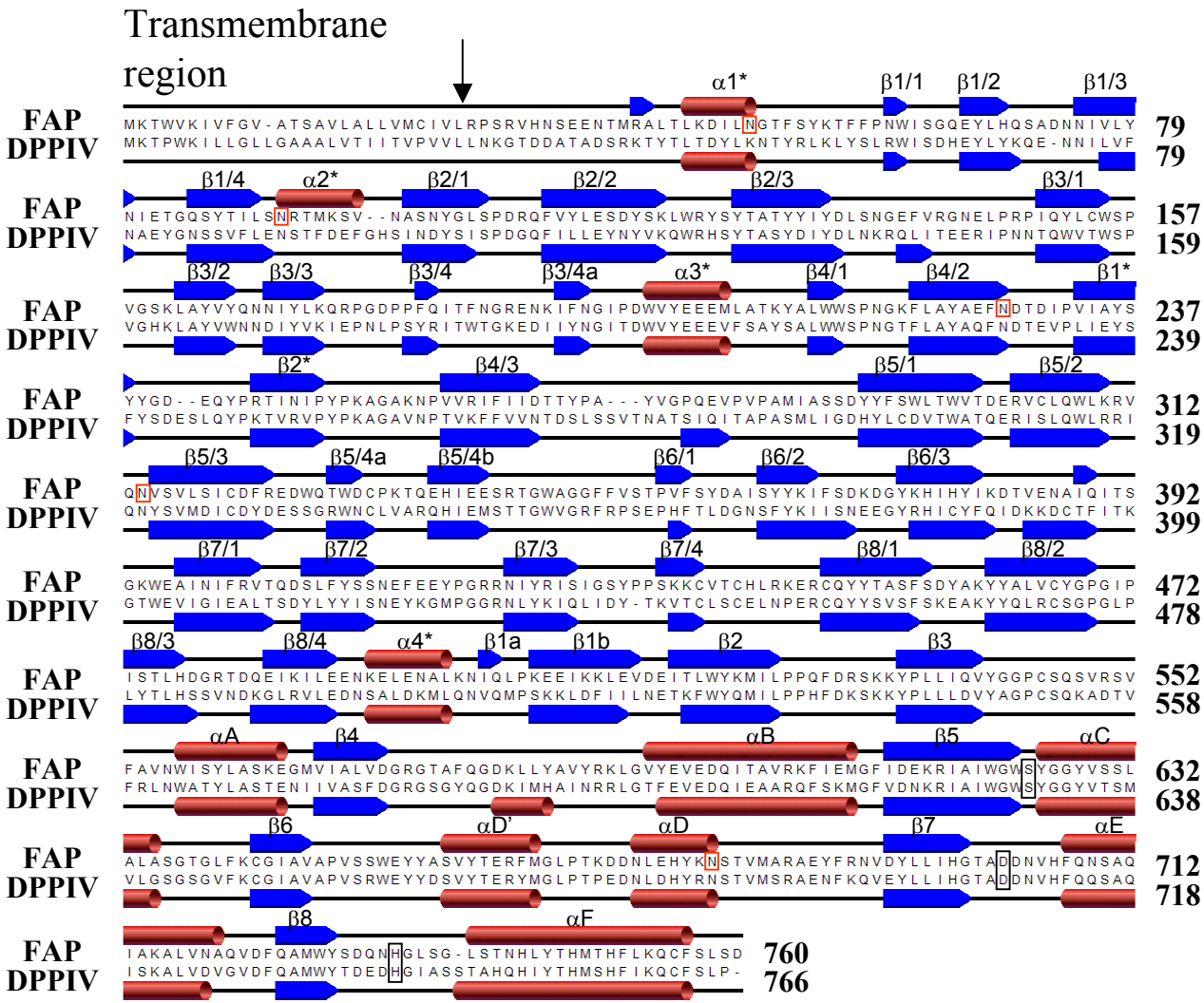
Data Collection

Wavelength (Å)	1.00
Spacegroup	P212121
Unit cell dimensions(Å)	a=70.30;b=152.58;c=214.89
Resolution (Å)	50.0 - 2.6
Unique Reflections	70612
Redundancy	3.4
Completeness (%)	97.8 (90.6)
I/σ(I)	12.0 (1.9)
R_{sym} [a]	0.095 (0.507)

Refinement

Resolution (Å)	50.0 – 2.6
Reflections used	66976
RMS Bonds (Å)	0.010
RMS Angles (°)	1.39
Average B value (Å^2)	27.0
R-value, R_{free} [b]	0.22, 0.28

[a] $R_{sym} = \Sigma_h\Sigma_j |<I(h)> - I(h)j| / \Sigma_h\Sigma_j <I(h)>$, where $<I(h)>$ is the mean intensity of symmetry-related reflections. [b] R-value = Σ | $|F_{obs}|$ - $|F_{calc}|$ | / Σ $|F_{obs}|$. R_{free} for 5% of reflections excluded from refinement. Values in parentheses are for the highest resolution shell.



Sequence alignment of FAPα and DPPIV. Arrows and cylinders are indicated above residues that are part of a β-strand or α-helix, respectively. The catalytic triad amino acid residues are indicated by black boxes, red boxes indicate glycosylation sites. The arrow indicates the start of the cloned ectodomain.